Electronic Supplementary Information (ESI)

SnS Nanoparticles Electrostatically Anchored on Three-dimensional N-doped Graphene as an Active and Durable Anode for Sodium Ion Batteries

Xunhui Xiong,[a] Chenghao Yang,[*a] Guanhua Wang,[a] Yuwei Lin,[b] Xing Ou,[a] Jeng-Han Wang,[b] Bote Zhao,[c] Meilin Liu,[c] Zhang Lin[a] and Kevin Huang[*d]

[a.] Guangzhou Key Laboratory of Surface Chemistry of Energy Materials, New Energy Research Institute, School of Environment and Energy, South China University of Technology, Guangzhou 510006, China.
E-mail: esyangc@scut.edu.cn; Tel: +86-803-39381203
[b.] Department of Chemistry, National Taiwan Normal University, Taipei, Taiwan 11677.
[c.] School of Materials Science & Engineering, Georgia Institute of Technology, Atlanta, GA 30332-0245, USA.
[d.] Department of Mechanical Engineering, University of South Carolina, Columbia, SC 29205, USA
E-mail: huang46@cec.sc.edu

Experimental methods

Materials synthesis: All the reagents used in the experiment were of analytical grade purity and used as received. Graphite oxide (GO) was prepared from graphite powder according to a modified Hummers' method. The as-obtained aqueous suspension of GO was diluted with deionized water under ultrasonication for 6 h to obtain an exfoliated graphene oxide (GO) suspension (~2 mg mL^{-1}). The functionalization of GO with PDDA was achieved as follows: 50 ml of GO solution was loaded into a round-bottom flask, followed by adding 10 mL of PDDA solution (1 wt %) and sonication for 1 h until no visible particulate. At the same time, 0.55 g of commercial SnS_2 was added to a 20 mL of $(NH_4)_2S$ solution under magnetic stirring until a clear and yellow solution was obtained. Then the yellow solution, PDDA

functionalized GO solution and dicyandiamide powders were mixed together by magnetic stirring and sonicated for another 1 h. The resultant dispersion was then frozen using liquid nitrogen, and subjected to a vacuum drying process for 24 h. Finally, the obtained porous powder was heated at 600 °C for 2 h under Ar atmosphere to yield SnS/3DNG hybrid. The SnS/3DG hybrid with the same content of graphene with SnS/3DNG and pure SnS were obtained from a similar process but without adding dicyandiamide powders or PDDA functionalized GO solution, respectively. The 3DNG was prepared by mixing PDDA functionalized GO solution and dicyandiamide powders, followed by freeze-drying and calcining. The $Na_3V_2(PO_4)_3$/C hybrid cathode was prepared by a method reported previously.[23]

Materials characterization: The Zeta potentials of GO and GO-PDDA suspensions were measured using a Zetasizer 3000HS (Malvern Instruments). The X-ray diffraction (XRD) patterns of samples were collected from a Rigaku D/max 2500 using Cu Kα radiation. Morphologies of prepared powders were investigated by a field-emission scanning electron microscopy (FESEM, Hitachi S-4800) and a transmission electron microscopy (TEM) and high resolution TEM (HRTEM) (TEM, JEM-2010, JEOL, 200 kV). Prior to TEM analysis, powders were ultrasonically dispersed in ethanol for 15 minutes. Surface characterization of elemental electronic states was examined by X-ray photoelectron spectroscopy (XPS, Thermo K-Alpha XPS spectrometer, Thermo Fisher Scientific) equipped with a monochromatic Al-Kα X-ray source (hν = 1468.6 eV). Raman spectroscopy was performed using a Renishaw RM1000 equipped with a He-Ne laser at an excitation wavelength of 633 nm (Thorlab

HRP-170) through a 20x/0.40 objective. The BET-specific surface areas were obtained from nitrogen adsorption–desorption isotherm at the boiling point of liquid nitrogen (77 K) using a Micromeritics ASAP 2020 analyzer.

Electrochemical tests: Coin-type half-cells were assembled in an Ar glove box to investigate the sodiation/desodiation behaviors of the prepared anodes. A homogenous slurry was obtained by mixing the as-prepared powders with super P and carboxymethyl cellulose (70:15:15 in weight) in deionized water, followed by coating it on a copper foil and dried at 100^{o}C under vacuum for 12 h. The typical thickness of the electrode is ~30 μm with a packing density of about 1.1~1.3 g cm^{-3}. The tailored Cu foil coated with active materials was used as work electrode with metallic sodium as the counter electrode, and glass fiber as the separator in a half-cell configuration. The electrolyte was a solution of 1 M $NaClO_4$ in propylene carbonate (PC) with 5% fluoroethylene carbonate (FEC) additive. Galvanostatic charge and discharge cycles were carried out using LAND CT2001A battery testing system (Wuhan, China) within a voltage range of 0.01-2.5 V based on the weight of the composite. Cyclic voltammetry (CV) measurements were made using IM6 electrochemical testing station running at 0.1 mV s^{-1} from the open circuit potential to 0.01 V and then back to 2.5 V.

Computational method

The density functional theory (DFT) calculations were performed by Vienna *Ab initio* Simulation Package (VASP).[24] The computational method employed generalized gradient approximation (GGA) with Perdew-Wang 1991 formulation (PW91) for the exchange-correlation function.[25] The valance electrons were expanded

by plane-wave basis with the cutoff energy at 600 eV to simulate the perodicity of the system and the core electrons were mimicked by the cost-effective pseudopotentials with projector-augmented wave method (PAW).[26] The Brillouin-Zone (BZ) integration was sampled by the Monkhorst-Pack scheme[27] with the sampling k-point at 0.05×2 (1/Å) interval in the reciprocal space. The spin-polarization was applied for all the calculations. The graphene sheet was modeled by a 5×5 supercell, while the nitrogen doped graphene was a thiophene-like structure by replacing one carbon to nitrogen atoms. All the atoms were fully relaxed during the calculation. The structural optimization and energetic calculation were carried out by the quasi-Newton method with an energetic convergence of 1×10^{-4} eV and gradient convergence of 1×10^{-2} eV. The Van der Waal correction conducted by DFT-D2 method of Grimme[28] was employed for the adsorption energy calculation.

Table S1 Zeta potentials (five measurements) of GO and PDDA-GO.

	1	2	3	4	5	Average
GO	-34.0	-33.8	-34.0	-34.3	-34.4	-34.1
PDDA-GO	60.9	61.3	61.5	61.6	61.2	61.3

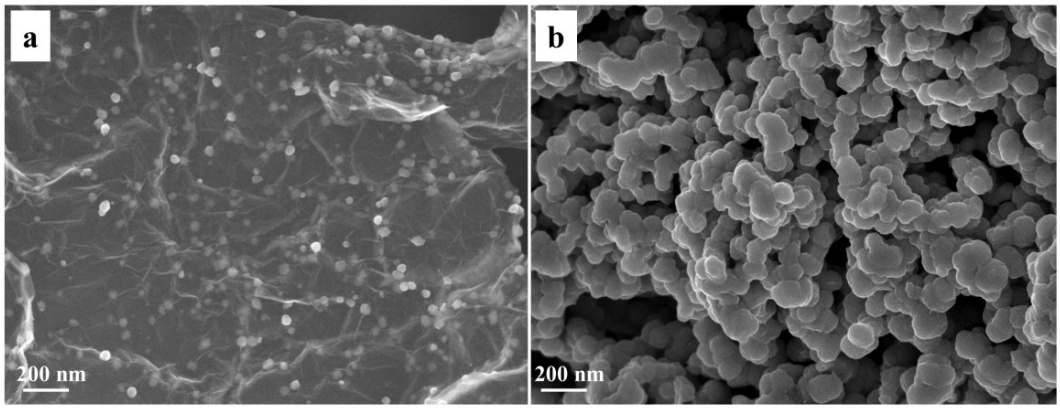

Figure S1 SEM images of (a) SnS/3DNG and (b) pure SnS prepared with similar method.

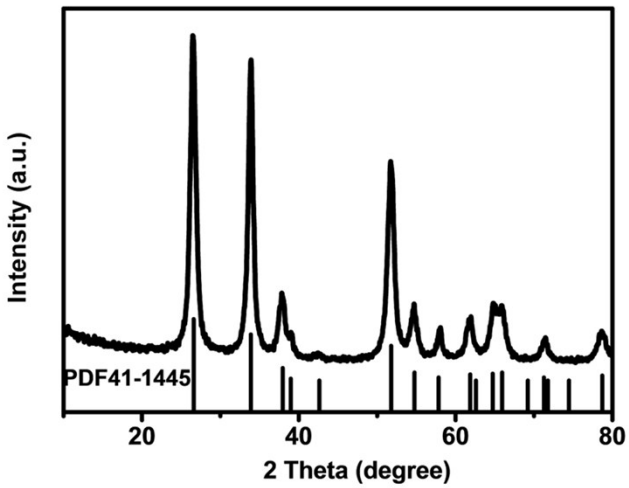

Figure S2 XRD patterns of powers obtained by calcining SnS/3DNG in air to 800 °C.

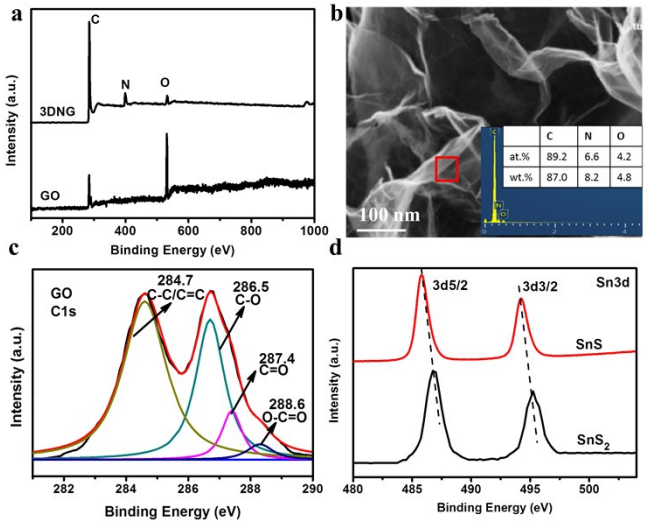

Figure S3 (a) Survey XPS spectra of GO and SnS; (b) TEM image of 3DNG and EDS analysis of the selected area; (c) high-resolution XPS spectra of C 1s GO; (d) high-resolution XPS spectra of Sn 3d in SnS and SnS_2.

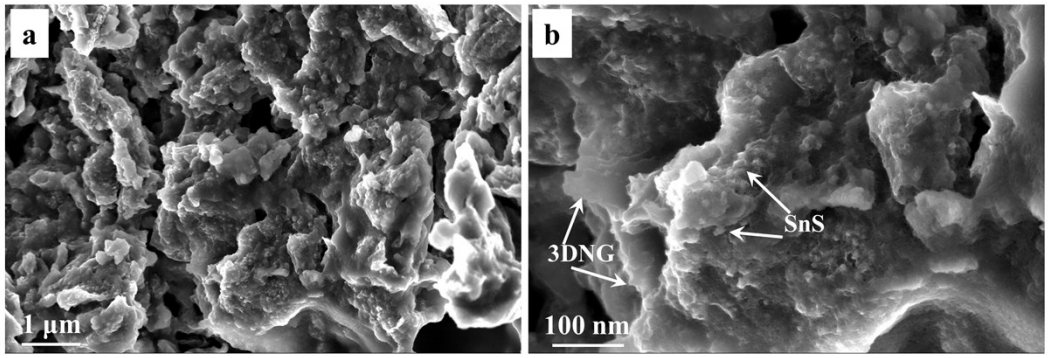

Figure S4 SEM images of SnS/N-doped graphene hybrid obtained by air drying method showing dense agglomerates.

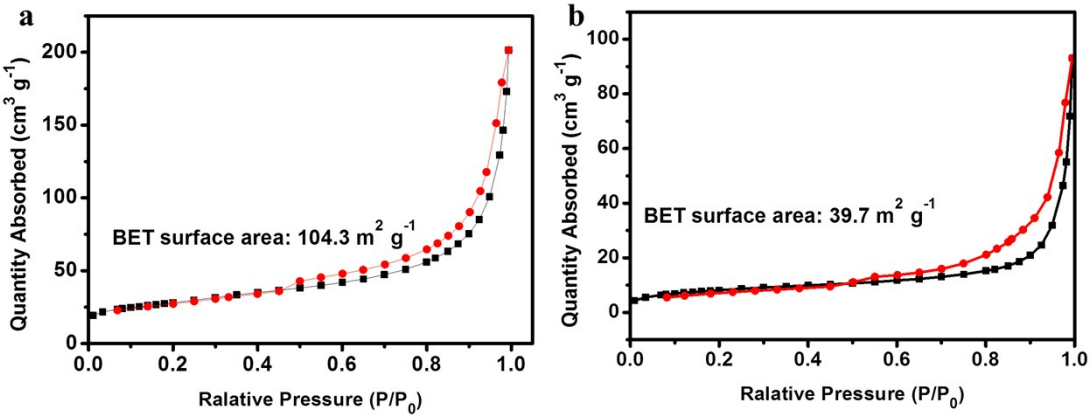

Figure S5 N_2 isotherms and calculated BET specific surface area of SnS/N-doped graphene: (a) freeze drying and (b) drying in air.

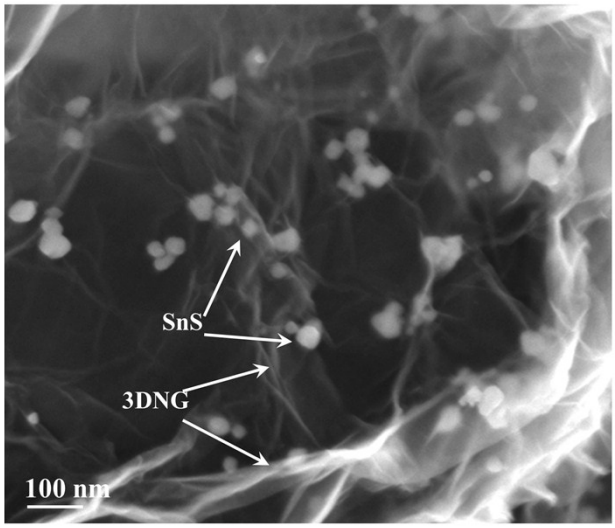

Figure S6 SEM image of SnS/3DNG showing agglomerated SnS nanoparticles on both sides of 3DNG.

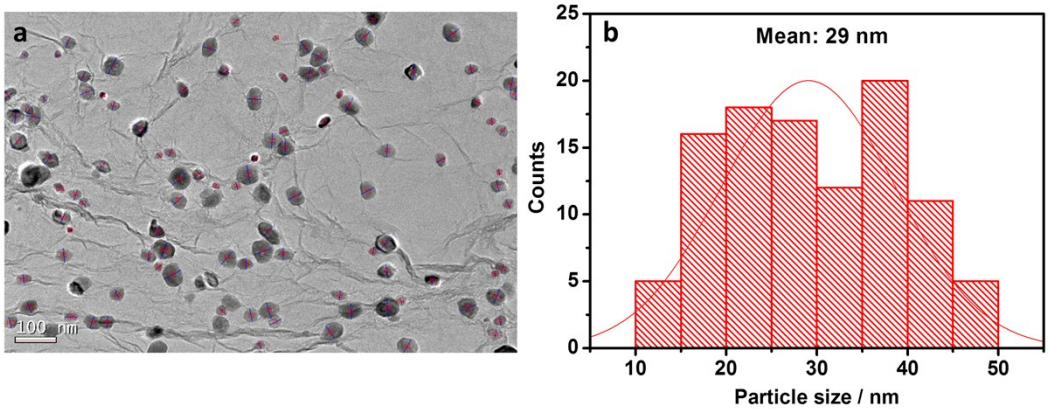

Figure S7 The particle size distribution of SnS on 3DNG.

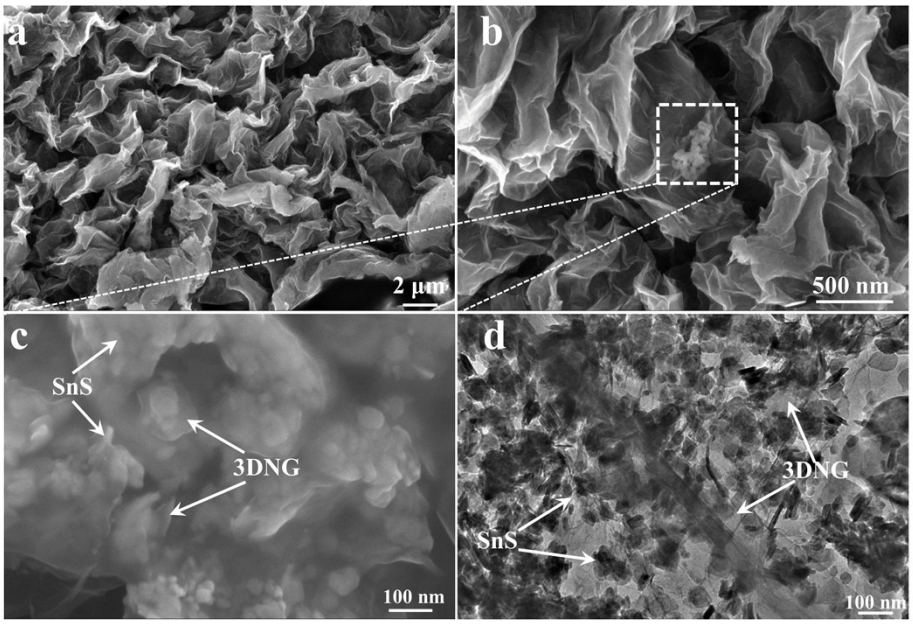

Figure S8 (a)-(b) SEM image (showing SnS unevenly distributed on graphene) and (c)-(d) TEM image of SnS/3DNG using unfunctionalized GO (graphene content in the hybrid is about 8.0 wt %), showing the SnS NPs are heavily agglomerated.

Table S2 Alloying reaction for the sodium-tin system in the ranges of 0.01-0.45V

Reaction	**Voltage range (V, vs. Na^+/Na)**
$Sn+Na \rightarrow Na_xSn$	0.41-0.45
$Na_xSn+Na \rightarrow \alpha\text{-}NaSn_2$	0.15-0.18
$\alpha\text{-}NaSn_2+Na \rightarrow Na_9Sn_4$	0.06-0.08
$Na_9Sn_4+Na \rightarrow Na_{15}Sn_4$	0.01-0.03

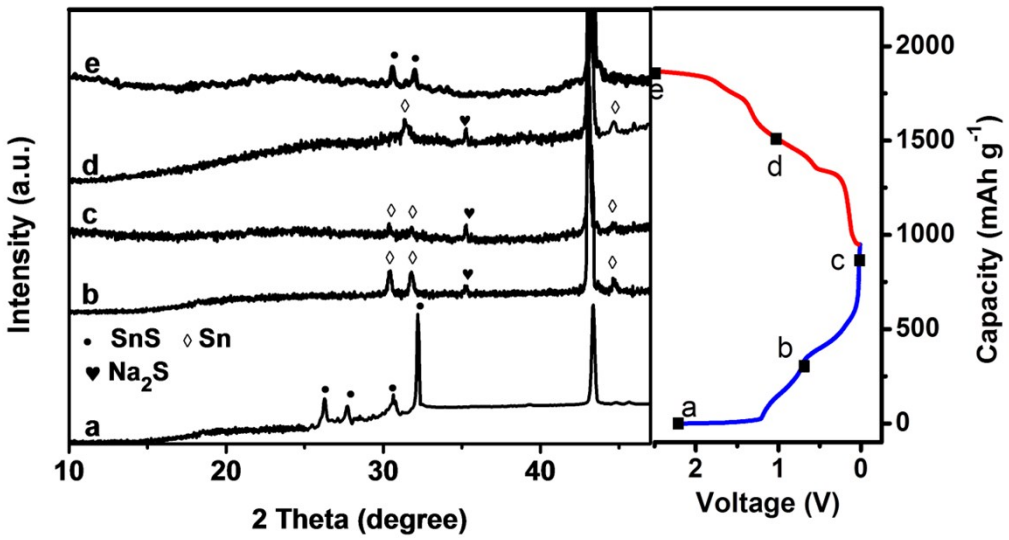

Figure S9 Ex situ XRD patterns of the SnS/3DNG anode collected at various states as indicated in the corresponding voltage profile: (a) fresh state; (b) after the first discharge to 0.8 V; (c) after the first discharge to 0.05 V; (d) after the first charge to 1.0 V, and (e) after the first charge to 2.4 V.

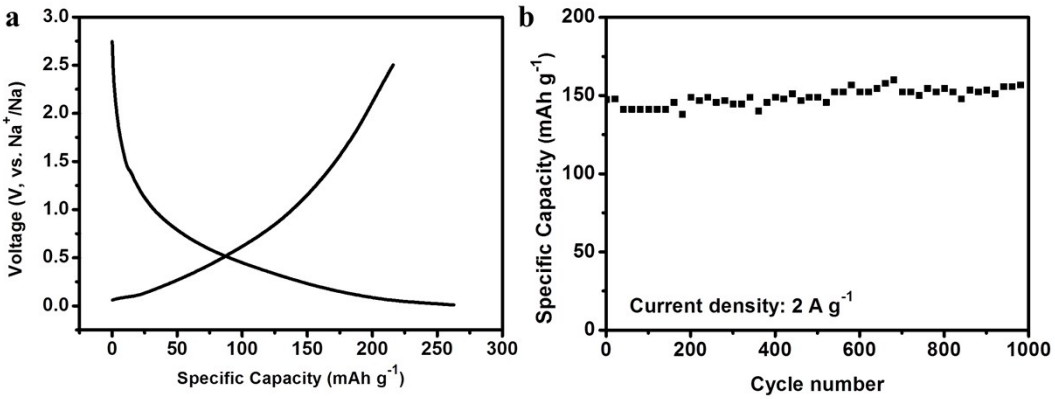

Figure S10 (a) The second charge-discharge curves of 3DNG at 100 mA g^{-1} and (b) the cycle performance at 2 A g^{-1}.

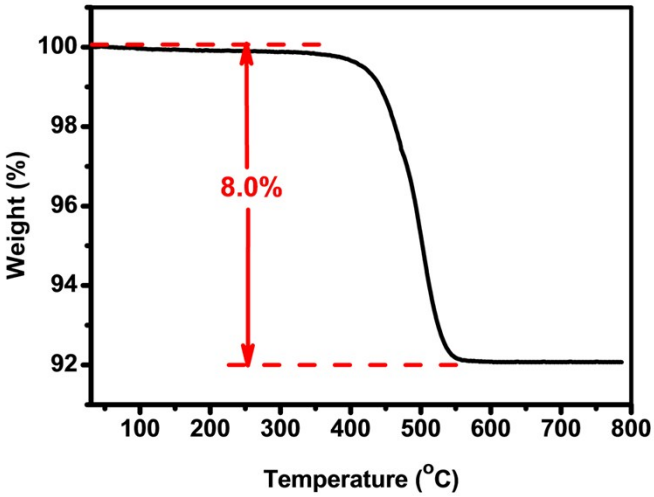

Figure S11 TG curve of the SnS/3DG hybrid in air with a heating rate of 2 °C min^{-1} and air flow of 100 mL min^{-1}.

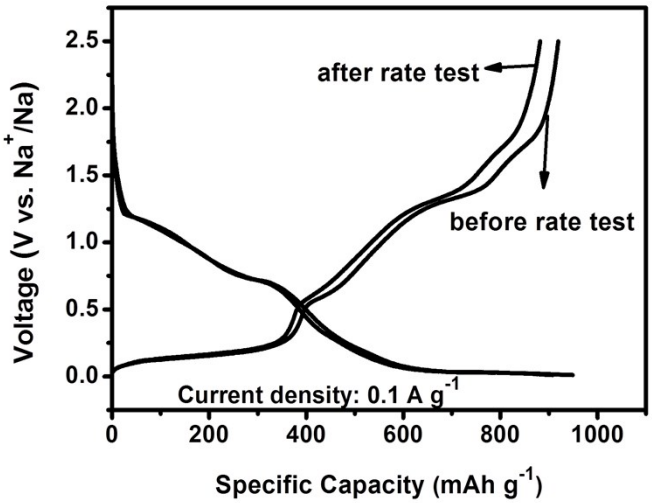

Figure S12 Comparison of the initial and after-rate-test charge-discharge profiles of SnS/3DNG anode at 0.1 A g^{-1}.

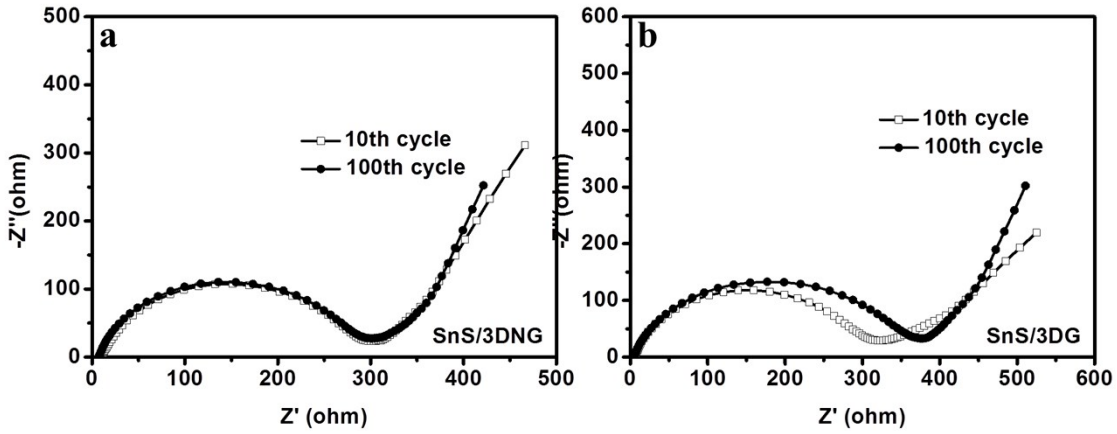

Figure S13 Nyquist plots of (a) SnS/3DNG and (b) SnS/3DG after different cycles at 0.1 A g^{-1} in a fully sodiation state (0.01V) from 1MHz to 10 mHz.

Table S3 Comparison of cycling performance of SnS/3DNG with previously reported Sn-based anodes for SIB

	Materials	Capacity	Retention	Reference
Ref. S1	SnS/graphene	308 mAh g^{-1}after 300 cycles at 7.29 A g^{-1}	88%	ACS Nano 2014, 8: 8323
Ref. S2	SnS Nano-honeycomb /graphene foam	1010 mAh g^{-1} after 200 cycles at0.1 A g^{-1}	88.1%	Nat. Comm.2016, 7, 12122
Ref. S3	SnS_2-RGO	500 mAh g^{-1}after 400 cyclesat1 A g^{-1}	84%	Adv. Mater. 2014, 26: 3854
Ref. S4	SnS_2/rGO	300 mAh g^{-1}after 1000 cycles at 0.8 A g^{-1}	61%	Adv. Funct. Mater. 2015, 25: 481
Ref. S5	SnS_2/amino-Functionalized graphene	480 mAh g^{-1}after 1000 cycles at 1 A g^{-1}	85%	*Energy Environ. Sci.*2016,9: 1430
Ref. S6	3D SnS/C	535 mAh g^{-1} after 300 cycles at 1 A g^{-1}	80%	*Adv. Sci.* 2015, 2, 1500200
Ref. S7	C@SnS/SnO_2@graphene	360 mAh g^{-1} after 500 cycles at 2.43 A g^{-1}	76%	*Angew. Chem. Int. Ed.* 2016, 55: 3408
Ref. S8	SnS-C	433 mAh g^{-1} after 50 cycles at 0.5 A g^{-1}	89%	Nano Research 2015, 8: 1595
Ref. S9	SnS-C	548 mAh g^{-1} after 80 cycles at 0.1 A g^{-1}	97%	J. Mater. Chem. A 2014, 2: 16424
Ref. S10	SnS@RGO	386 mAh g^{-1} after 100 cycles at 0.1 A g^{-1}	94%	J. Power Sources 2015, 293: 784
Ref. S11	exfoliated-SnS_2/graphene	610 mA h g^{-1}after 300 cycles at 0.2 A g^{-1}	100%	Nanoscale2015, 7: 1325
Ref. S12	SnO_2-RGO	330 mA h g^{-1}after 150 cycles at 0.1 A g^{-1}	81.3%	J. Mater. Chem. A 2014, 2: 529
Ref. S13	8-Sn@C	415 mAh g^{-1}after 500 cycles at 1 A g^{-1}	97.6%	Adv. Func. Mater. 2015, 25: 214
	SnS/3DNG	509.9 mAh g^{-1}after 1000 cycles at 2 A g^{-1}	87.1%	Our work

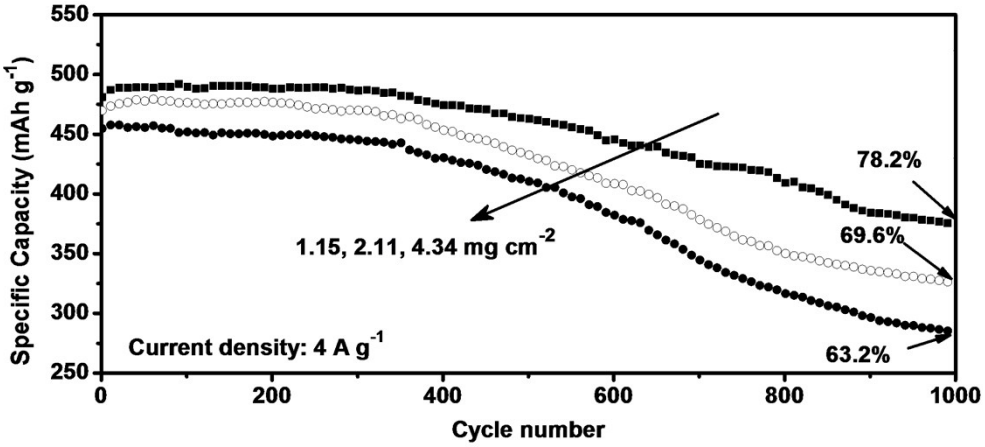

Figure S14 The capacities of the SnS/3DNG electrode with different active materials loading at 4 A g^{-1}.

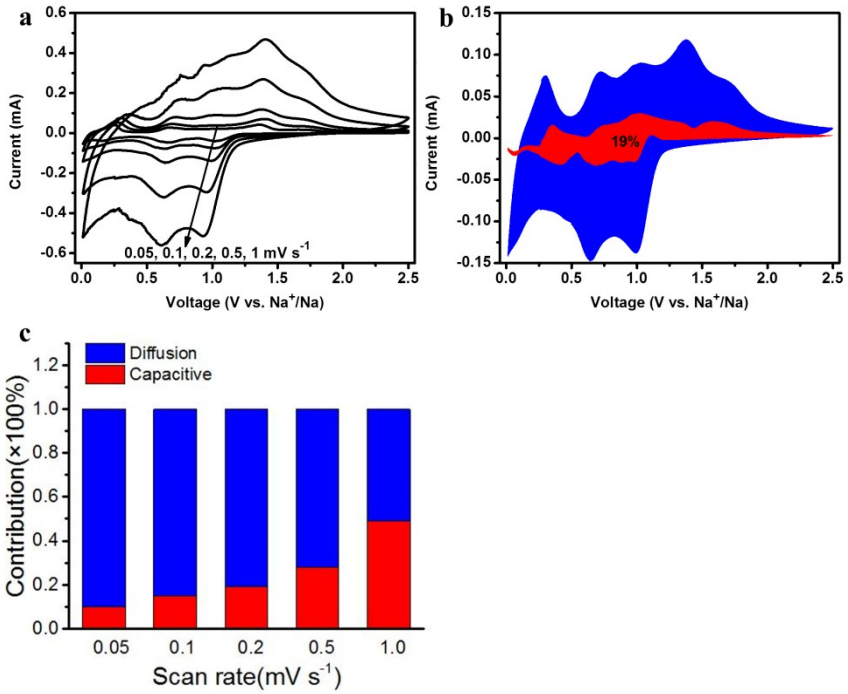

Figure S15 (a) CV curves of SnS/3DNG obtained at different scan rates; (b) capacitive (red) and diffusion-controlled (blue) contributions to charge storage of SnS/3DNG at 0.2 mVs^{-1}; (c) normalized contribution ratio of capacitive (red) and diffusion-controlled (blue) capacities at different scan rates.

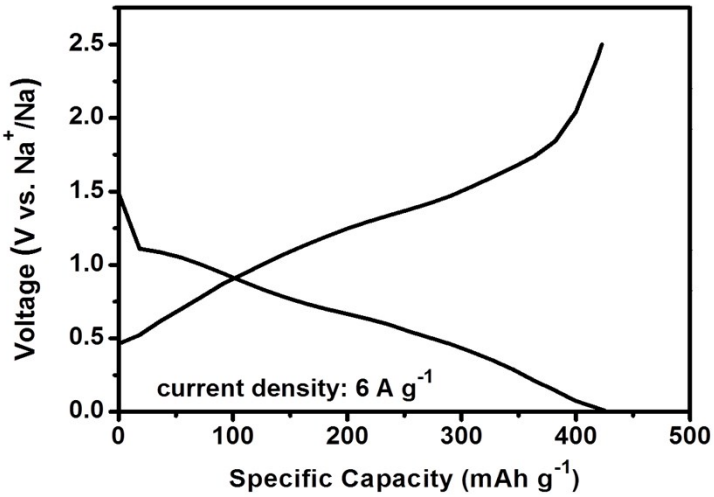

Figure S16 The charge-discharge profile of SnS/3DNG anode at 6A g^{-1}, showing a plateaus at 1.1 V, followed by a long slope.

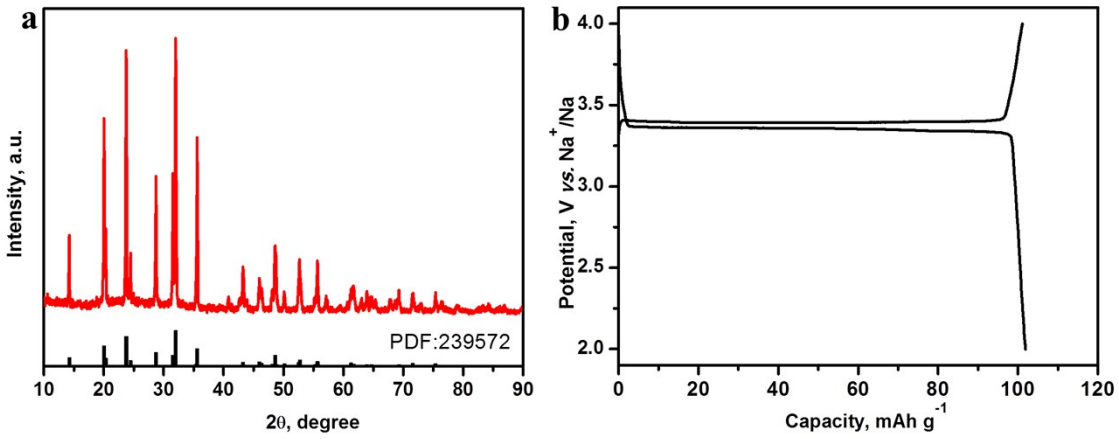

Figure S17 (a) XRD pattern of $Na_3V_2(PO_4)_3$/C composite and (b) charge/discharge profiles at current density of 0.2 A g^{-1}.

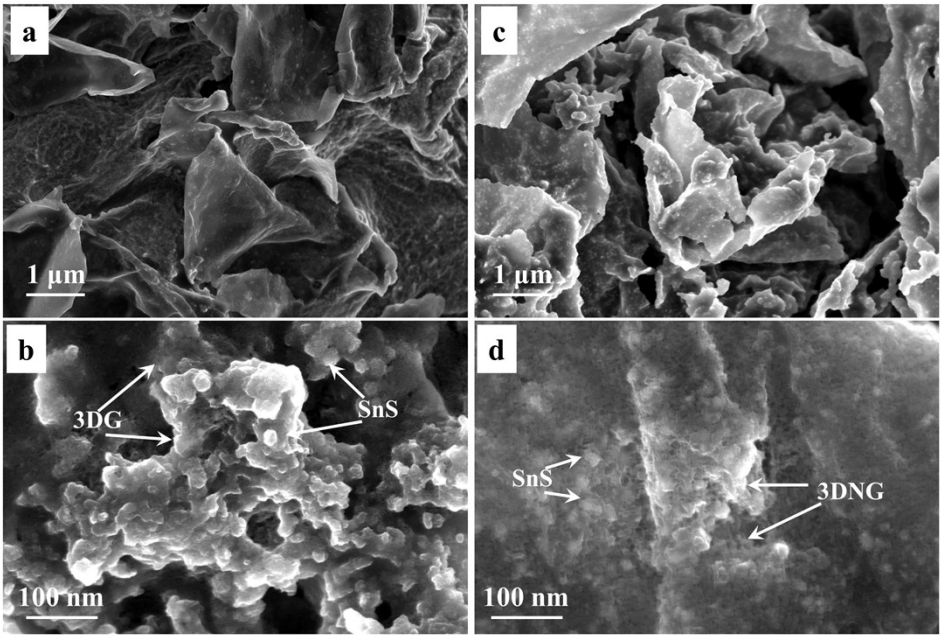

Figure S18 (a)-(b) SEM images of SnS/3DG and (c)-(d) SnS/3DNG after 1,000 cycles at 2 A g^{-1}

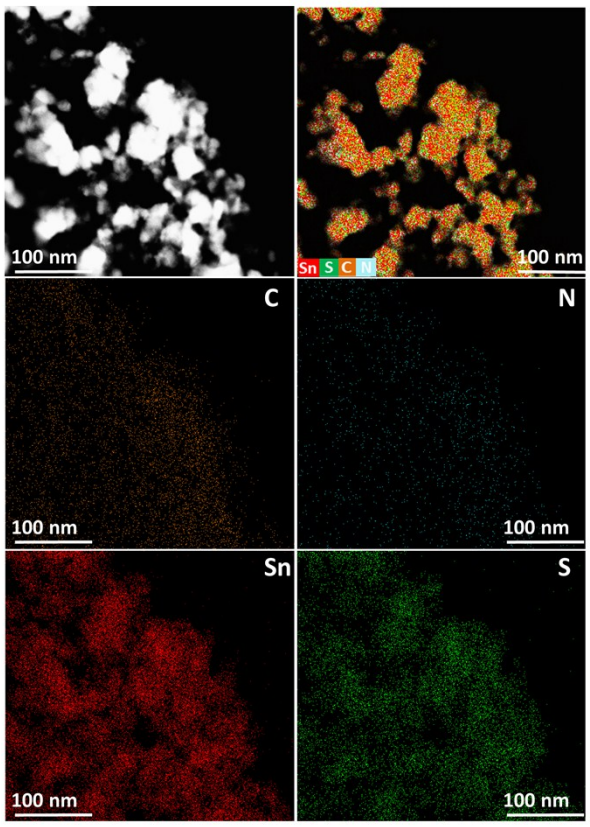

Fig. S19 TEM image and the corresponding C, N, S, and Sn elemental maps of the SnS/3DNG electrode after 1,000 charge/discharge cycles.

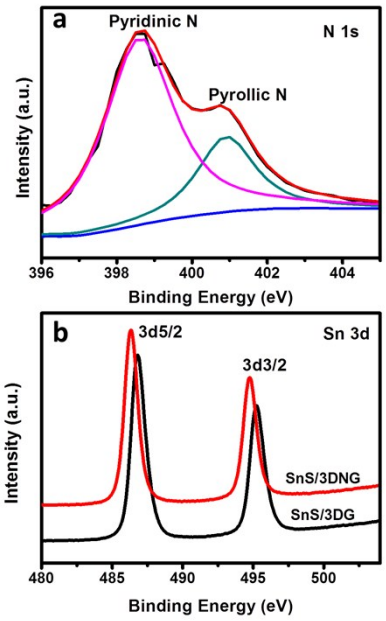

Fig. S20 High-resolution XPS spectra of N 1s and Sn 3d in SnS/3DNG. The negative shift of Sn 3d peaks in binding energy, indicating electron clouds still being biased from 3DNG to SnS after extensive cycling.